Design and Fabrication of Photonic Crystal Nano-Beam Resonator: Transmission Line Model

M. Miri, M. Sodagar, K. Mehrany, A. A. Eftekhar, A. Adibi, and B. Rashidian

***Abstract*—We present a new method for modeling and design of photonic crystal nano-beam resonators (PCNBRs) based on cascaded transmission lines. The proposed model provides an accurate estimate of the PCNBRs properties such as resonance wavelength and quality factor (Q) with much smaller computation cost as compared to the brute-force numerical methods. Furthermore, we have developed a straightforward technique for the design of high-Q PCNBRs based on resonance modes with Gaussian electromagnetic field profiles. The results obtained by using the proposed transmission line model are compared against numerical and experimental results and the accuracy of the model is verified. The proposed model provides an insight to silicon cavity design and significantly reduces computational burden.**

***Index Terms*—Nano-beam resonators, photonic crystals (PCs), transmission line (TL) model.**

I. Introduction

PHOTONIC crystal (PC) nano-beam resonators (PCNBR)—thanks to their high quality factor and low mode volume—are among the promising candidates for different applications ranging from linear and nonlinear optical signal processing [1], [2] to cavity quantum electrodynamics [3], [4]. It is no wonder that they have been the subject of many investigations in the past decade [1]–[10]. In particular, usage of PCNBR for nano-laser applications has been notable [11]–[13]. Quality factors as high as 7×10^5 for air bridge nano-beams [6], and mode volumes as low as $0.2(\lambda/2n)^3$ for slotted nano-beams [7] are reported in the literature. Since PCNBR is formed by introducing either local or distributed defect in an otherwise periodic waveguide structure, a fast and efficient design strategy is highly desirable to find the proper defect that can fully exploit the potentials of PCNBRs.

There are only two prominent design strategies hitherto reported. One is based on the Fabry–Perot model [14], and the other on mode gap modulation [6], [8], [10], and [15]. The former strategy tries to increase the quality factor by increasing the reflection at the boundary of the resonant region (as if the PCNBR is a simple Fabry–Perot resonator). Unfortunately, the radiation loss, which is inevitably incurred because of the unwanted sharp transitions of the electromagnetic field at the boundary of the resonant region, is neglected in this approach. Therefore, the achievable quality factor when the cavity is simply formed by introducing a local defect in a 1-D periodic waveguide is not usually ultrahigh. It can be substantially improved by fine tuning of the optical properties of the reflecting regions (e.g., by changing the radii and locations of the holes when the reflecting regions are made of PC waveguide formed by perforating a silicon waveguide) [16], [17]. The fine tuning of the reflecting regions is however a time consuming numerical procedure. The latter strategy, on the other hand, tries to blur the unwanted sharp field transitions by introducing the appropriate distributed defect that can reduce the radiation loss and increase the quality factor substantially. It is shown that the appropriate distributed defect should have a Gaussian-like field profile. Realization of the desired Gaussian-like field profile is possible via modulation of the band edge of PC waveguide modes in the distributed defect region and is not as expensive as fine tuning of the optical properties of the reflecting regions in the former strategy. Nevertheless, the extraction of the appropriate distributed defect profile requires running brute-force numerical simulations, e.g., 3-D finite difference time domain (FDTD) method, which happens to be very time-consuming task that complicates the adoption of this strategy.

The latter strategy is adopted in this paper. Conventionally, the desired Gaussian-like field profile is realized by linearly increasing the mirror strength along the reflecting region [15]. This can be achieved by decreasing the radii of the air holes when the reflecting regions are made of PC waveguide formed by perforating a silicon waveguide. Extraction of mirror strength in the reflecting region is however a painstaking step and needs 3-D band diagram simulations. Since pursuing such an approach takes about tens of hours on an ordinary desktop computer, a more efficient alternative is in want. Here, the standard transmission line (TL) theory is invoked to extract the appropriate distributed defect profile that can realize the desired Gaussian-like field profile. TL models have been proposed as a successful approximate tool for analysis of 2-D periodic structures (2D PCs) that are uniform along the third dimension [18], [19]. These structures form a 2-D computation problem. To the best of our knowledge, no such model is reported for analysis of the similar PC structures that are not uniform along the third dimension, i.e., when these structures form a 3-D computation problem. The existing TL models of 2-D PC structures cannot be straightforwardly extended to include the out-of-plane

Manuscript received May 17, 2013; revised October 25, 2013; accepted November 6, 2013. Date of publication November 13, 2013; date of current version November 29, 2013.

M. Miri, K. Mehrany, and B. Rashidian are with the Department of Electrical Engineering, Sharif University of Technology, Tehran, Iran (e-mail: m101miri@gmail.com; mehrany@sharif.ir; rashidia@sharif.edu).

M. Sodagar, A. A. Eftekhar, and A. Adibi are with the Department of Electrical Engineering, Georgia Institute of Technology, Atlanta, GA 30332 USA (e-mail: majidsodagar@gmail.com; eftekhar@ece.gatech.edu; ali.adibi@ece.gatech.edu).

Color versions of one or more of the figures in this paper are available online at http://ieeexplore.ieee.org.

Digital Object Identifier 10.1109/JLT.2013.2290947

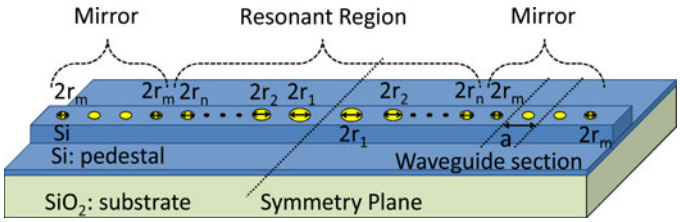

Fig. 1. Schematic view of a typical silicon PCNBR.

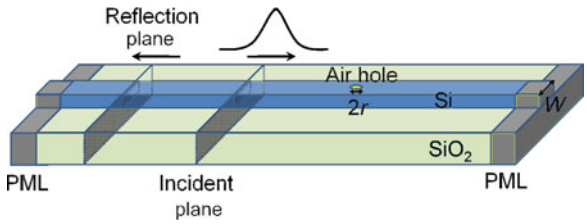

Fig. 2. FDTD simulation structure for the calculation of reflection coefficient. Waveguide section is illuminated by a rib waveguide mode while perfectly matched layer (PML) boundary conditions are used at both ends of the waveguides and reflection coefficient is calculated at indicated plane.

inhomogeneity and finite thickness of 3-D structures. This is carried out in this paper and the PCBNR is modeled by a TL circuit. The here-proposed TL model can considerably reduce the runtime of the process.

The structure of this paper is as follows. First, the details of modeling PCNBRs by TL are given in Section II. The PCNBR is divided to cascaded PC waveguide sections. Each section is modeled by a TL segment of the same length. The propagation constant and characteristic impedance of the TL segment are obtained by solving a set of equations that relates the numerically extracted reflection coefficient of the waveguide section to the sought-after parameters of the TL segment. Once the parameters of the TL segment modeling each PC waveguide section are obtained, the PCNBR is automatically modeled by cascaded TL segments. The accuracy of the proposed TL model in extraction of the resonance wavelength and its corresponding quality factor is verified by analysis of a typical Fabry–Perot PCBNR. The zero frequency of the imaginary part of the network's total impedance and its corresponding frequency bandwidth give the resonance wavelength and its corresponding quality factor, respectively. It is shown that the results obtained by the proposed model are as accurate as those obtained by brute force numerical method. In Section III, the proposed model is employed to design resonators of very high quality factor. To this end, the field profile of the PCNBR mode is first related to the voltage distribution within the cascaded TL model. The parameters of the TL segments are then obtained in such a manner that the voltage distribution becomes Gaussian. In Section IV, the designed structure is fabricated and characterized. The obtained results demonstrate the accuracy and efficiency of the proposed TL model for analysis and design of PCBNRs. Finally, the conclusions are made in section V.

II. Transmission Line Model for PCNBR

Without loss of generality, we focus on PCNBR that is formed by perforating equidistant circular air holes in a silicon rib waveguide. The schematic of such a structure is shown in Fig. 1. The resonant region is formed by changing the radii of $2n$ holes sandwiched between two PC waveguide mirrors, whose periodicity and radii of holes are denoted by a and r_m, respectively. In accordance with Fig. 1, there is a plane of symmetry around which the radii of holes within the resonant region are shown by $r_i, i = 1, 2, \ldots, n$.

Given that the distance between the center of two adjacent holes is a, the PCNBR in Fig. 1 can be regarded as a cascaded sequence PC waveguide sections with length a; each with its specific PC hole radius (see Fig. 1). As mentioned earlier if a TL model is developed for each PC waveguide section, then the PCNBR can be modeled by cascaded TL segments. In the next section, we use cascaded TL model to calculate the PC waveguide transmission/reflection.

A. Transmission Line Model for PC Waveguide Sections

Consider a typical waveguide section whose length is a, and has a circular air hole of radius r. Two steps are to be taken to replace such a waveguide section by a TL segment. The propagation constant of the TL segment γ and its impedance z_c are to be determined. In the first step, the reflection of the waveguide section when it is created by perforating an air hole of radius r within the silicon rib waveguide is numerically extracted by using 3-D FDTD. Fig. 2 shows the details of FDTD reflection calculation. The waveguide section is illuminated by a rib waveguide mode while perfectly matched layer boundary conditions are used at both ends of the waveguides and reflection coefficient is calculated at the plane that is indicated in Fig. 2. The rib waveguide mode in the FDTD simulation is modulated by a temporal Gaussian envelope and therefore reflections is calculated at a range of frequencies.

For each PC waveguide section two simulations should be performed to extract two unknown parameters γ and z_c. These two simulation steps are shown in Fig. 3. In following calculations all impedances are normalized in respect to characteristic impedance of the rib waveguide. In accordance with Fig. 3(a), if the waveguide section is to be replaced by a TL segment of length a then the reflection coefficient Γ_1 can be written in terms of the propagation constant γ and the normalized characteristic impedance z_c:

$$\Gamma_1 = \frac{z_{\mathrm{in}(1)} - 1}{z_{\mathrm{in}(1)} + 1} \tag{1}$$

where $z_{\mathrm{in}(1)}$ is the normalized input impedance of the TL segment that models the waveguide section

$$z_{\mathrm{in}(1)} = z_c \frac{1 + z_c \tanh \gamma a}{z_c + \tanh \gamma a}. \tag{2}$$

In the second step, the reflection coefficient of the waveguide section when it is cascaded by the same waveguide section is numerically extracted. In accordance with Fig. 3(b), the cascaded waveguide sections are to be replaced by a TL segment of length $2a$. This time, the reflection coefficient of the structure

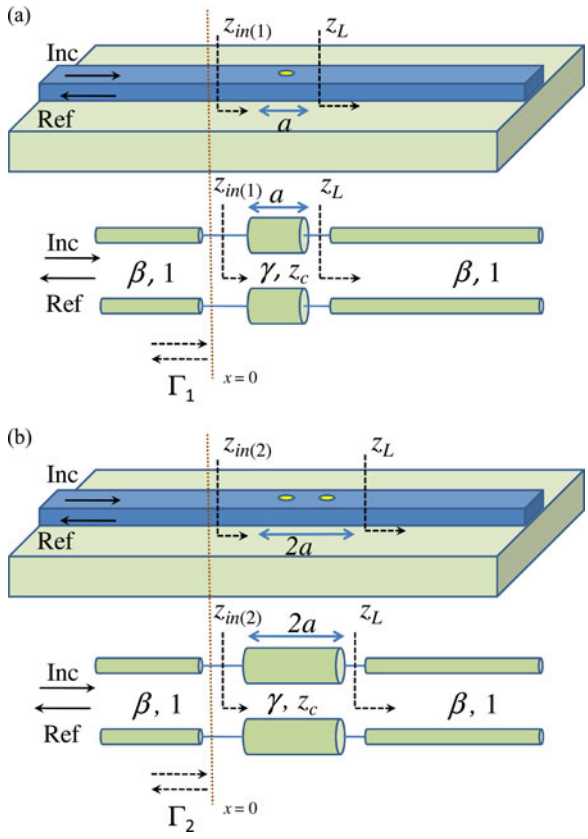

Fig. 3. Extraction of the TL model for a typical waveguide section of the PCNBR shown in Fig. 1. (a) The first step in extraction of the model parameters. (b) The second step in extraction of the model parameters.

Γ_2 can be written as

$$\Gamma_2 = \frac{z_{\mathrm{in}(2)} - 1}{z_{\mathrm{in}(2)} + 1} \tag{3}$$

where $z_{\mathrm{in}(2)}$ is the normalized input impedance of the TL segment that models the cascaded waveguide sections

$$z_{\mathrm{in}(2)} = z_c \frac{1 + z_c \tanh 2\gamma a}{z_c + \tanh 2\gamma a}. \tag{4}$$

Given that the reflection coefficients Γ_1 and Γ_2 are numerically extracted, the propagation constant γ and the normalized characteristic impedance z_c of the TL model of the waveguide section can be straightforwardly obtained by solving the following set of equations:

$$z_c \frac{1 + \tanh^2 \gamma a + 2 z_c \tanh \gamma a}{z_c + z_c \tanh^2 \gamma a + 2 \tanh \gamma a} = \frac{1 + \Gamma_2}{1 - \Gamma_2} \tag{5.a}$$

$$z_c \frac{1 + z_c \tanh \gamma a}{z_c + \tanh \gamma a} = \frac{1 + \Gamma_1}{1 - \Gamma_1}. \tag{5.b}$$

This nonlinear equation system can be solved by using numerical methods. Here we have used MATLAB software to solve these equations. It is worth noting that for $r = 0$, when no hole is perforated in the silicon rib waveguide, the above-mentioned set of equations fail to render the normalized characteristic impedance and the propagation constant. To resolve this issue, other facts are to be used. Since no reflection is expected when $r = 0$, the normalized characteristic impedance of the TL model should be $z_c = 1$. Moreover, since the electrical length of the TL model for $r = 0$ should not be different from the electrical length of the silicon rib waveguide, the propagation constant of the TL model γ should be equal to that of the silicon rib waveguide β. Calculated propagation constant and characteristic impedance for PC waveguide sections considered in following examples are complex number. This is in agreement with the fact that since desired frequency range is in the photonic mode gap of PC waveguides the equivalent TLs should have complex characteristics impedances and propagation constants. In the next section the proposed TL model will be used for designing PCNBRs based on algorithm discussed in Section II. But before considering the design problem, accuracy of the proposed model is tested by modeling a Fabry–Perot based PCNBR in the following section.

B. Modeling of the PCNBR Using Transmission Line Approach

To demonstrate how the TL model of PC waveguide sections can be employed to model PCNBR and to verify the accuracy of the proposed model, a typical Fabry–Perot PCNBR is considered. Here the TL model for PC waveguide sections will be used to calculate resonance wavelength and quality factor the Fabry–Perot PCNBR. These values are then compared against results of 3-D FDTD simulations. The Fabry–Perot PCNBR is made by two PC waveguide mirrors that sandwich a resonant region with no holes. In accordance with the previous section, the waveguide sections of the Fabry–Perot PCNBR—a silicon rib waveguide together with PC waveguide mirrors- are substituted by their corresponding TL models. This is shown in Fig. 4(a). It is assumed that the silicon rib waveguide in which the Fabry–Perot PCNBR is to be fabricated has thickness of $h =$ 240 nm, width of $w = 500$ nm, and pedestal layer of thickness $t = 50$ nm. The PC waveguide mirrors have five equidistant air holes of radius $r = 80$ nm and $a = 350$ nm. The length of the resonant region is $L = 1.1$ μm. To extract the resonance wavelength and the quality factor of such a typical PCNBR by using the proposed TL model, the normalized impedance of PC waveguide z_c and the propagation constants of PC waveguide and the silicon rib waveguide γ and β are to be calculated first. Then, the resonance condition of the TL model is to be satisfied. At the resonance wavelength, the imaginary part of the total impedance of the network should be zero [20]

$$\mathrm{Im}\{z_{\mathrm{tot}}\} = 0;\ z_{\mathrm{tot}} = z_L + z_R \tag{6}$$

where z_R and z_L are the normalized impedances seen at the right- and left-hand sides of an arbitrary interface in the circuit, respectively. Here, the chosen interface corresponds to the boundary between the resonant region and the PC waveguide mirror

$$z_L = \frac{z_{\mathrm{load}} + j \tan \beta L}{1 + j z_{\mathrm{load}} \tan \beta L} \tag{7.a}$$

$$z_R = z_{\mathrm{load}} = z_c \frac{1 + z_c \tanh 5\gamma a}{z_c + \tanh 5\gamma a}. \tag{7.b}$$

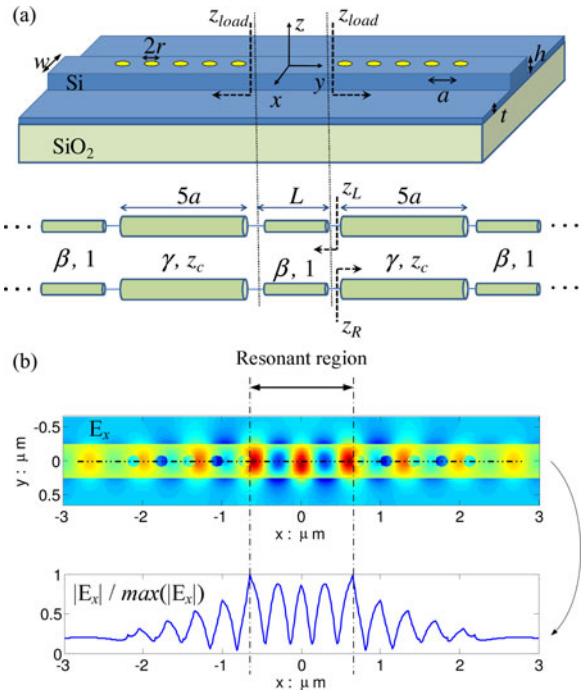

Fig. 4. (a) Schematic view of a typical Fabry–Perot PCNBR together with its equivalent TL model. (b) The x component of the electric field profile (E_x) of the resonance mode extracted from FDTD and absolute value of E_x in $x = 0$ along the resonator.

Therefore by knowing propagation constant and characteristic impedance of the PC waveguide sections we can calculate z_R, z_L, and $z_{\rm tot}$ from above equations. However since the proposed TL model is a frequency domain model we need to perform a frequency sweep and calculate $z_{\rm tot}$ for a range of frequencies to find the resonance frequency at which equation (6) is satisfied. Our calculations show that the resonance condition is satisfied when the wavelength of light at free space is $\lambda_0 = 1548.60$ nm. At this wavelength, the normalized impedance of PC waveguide is $z_c = 0.0132 - 0.0100\,i$, and the propagation constants of PC waveguide and the silicon rib waveguide are $\gamma = 3.0971 \times 10^4 + 1.5914 \times 10^4 i$ and $\beta = 1.0164 \times 10^7$, respectively. The corresponding quality factor can then be easily obtained by finding the full-width at half maximum of the total impedance $z_{\rm tot}$ [20]. From bandwidth of total impedance at the abovementioned resonance wavelength the quality factor of the PCNBR is found to be $Q = 134.47$.

Using the brute-force 3-D FDTD, the resonance wavelength and the quality factor of the same PCNBR are $\lambda_0 = 1553.12$ nm, and $Q = 133.15$, respectively. These results are obtained by using the commercially available Lumerical software. It can be seen that the error of using the proposed model in calculation of the resonance wavelength and quality factor is below 0.3%, and 1%, respectively.

As it mentioned earlier one reason to have a rather low value for the quality factor in the Fabry–Perot PCNBR is the sharp transition of the electric field at the boundaries of the resonant region. This is shown in Fig. 4(b), where a snap shot of the x component of the resonant electric field profile; E_x, is plotted together with its absolute value at $x = 0$ and $z = 0$. The sharp transition at the boundary between the resonant region and the PC waveguide mirror is noticeable.

III. PCNBR Design

Given that the proposed TL model provides the resonance wavelength and quality factor of the PCNBR in a simple, quick and efficient manner, standard optimization procedures can be followed to design the desired PCNBR. Still, finding the optimum PCNBR having the maximum possible quality factor at a specified resonance wavelength requires a rather complex optimization procedure and is not a straightforward task. Here, a more heuristic approach based on physical principles is followed instead of pursuing a standard optimization technique in a blind manner. The most appropriate values for the geometrical parameters of the silicon rib waveguide and of the PC waveguide mirror are obtained to ensure that the radiation loss of the structure reaches the minimum possible level. Then, the resonant region is designed in two steps. First, air hole radius of the innermost PC waveguide section is chosen to support the desired resonance wavelength. Since the resonance wavelength of the PCNBR principle mode is close to the photonic band edge of the innermost PC waveguide section [15], the air hole radius is found by bringing the spectral position of the photonic band edge near the desired resonance wavelength. Second, air hole radii of the outer PC waveguide sections within the resonant region are found by trying to suppress the field profile mismatch between PC waveguide mirrors and the resonant region. In this way, the unwanted radiation loss is reduced. Since the least mismatch is observed when the electromagnetic field energy is optimally confined around a specific wave vector point in the momentum space [21], [22], the unknown radii of the air holes within the resonant region should support a Gaussian electromagnetic field profile [15], [21]. This step can be considerably expedited, when the proposed TL model is employed.

The width of the silicon rib waveguide in the to-be-designed PCNBR should be large enough to ensure that the waveguide mode is well below the light line (to reduce the radiation loss) while it should be small enough to ensure that the waveguide remains single mode. Since the PCNBR is to be fabricated on a SOI wafer whose silicon thickness is $h = 240$ nm and since the pedestal layer has a $t = 50$ nm thickness, the width of the waveguide can be $w = 500$ nm to support a single propagating mode around the communication wavelength 1550 nm lying well below the light line.

The periodicity of the PC waveguide mirrors a should be small enough to ensure that the edge of the Brillouin zone π/a is farther than the edge of the radiation zone $2\pi/\lambda_0$ [21], [22]. However, it cannot be too small otherwise the fabrication process becomes complicated. The periodicity of the to-be-designed PCNBR is here set to $a = 340$ nm. The air hole radius of the PC waveguide mirror should be $r_m = 80$ nm to make sure that the desired communication wavelength 1550 nm is at the center of the photonic gap. This is shown in Fig. 5, where the band structure of the PC waveguide mirrors and the desired resonance wavelength $\lambda_0 = 1550$ nm are depicted.

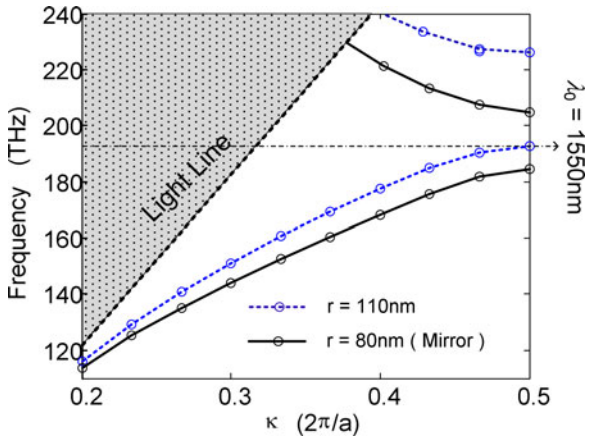

Fig. 5. Band structure of the photonic crystal waveguide mirrors with r_m = 80 nm (black solid lines), and the innermost photonic crystal waveguide section with r_1 = 110 nm (blue dashed lines).These values are chosen to make sure that the desired communication wavelength 1550 nm will be at the center of the photonic gap of PC waveguide mirror and at the band edge of innermost PC waveguide sections.

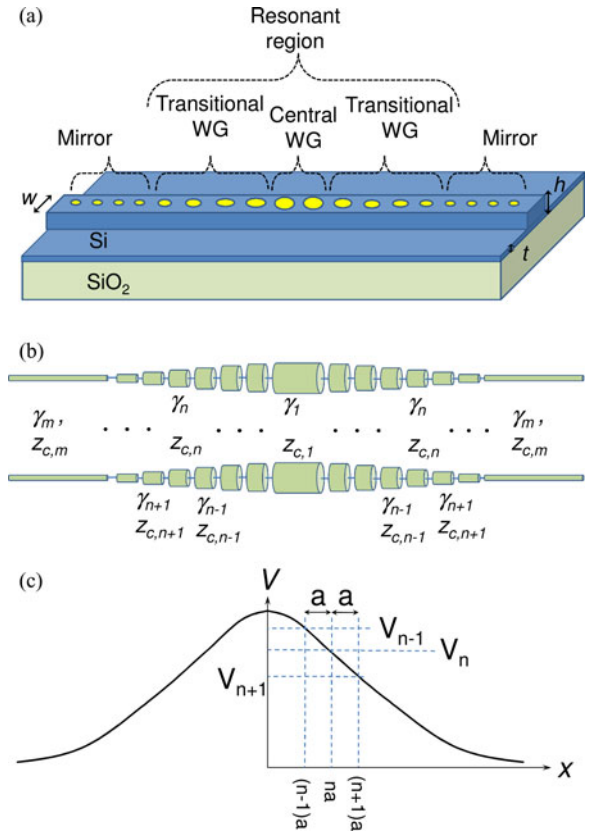

Fig. 6. (a) Schematic view of the PCNBR. (b) TL model of the PCNBR. (c) The desired Gaussian voltage distribution.

Now that the silicon rib waveguide and the PC waveguide mirrors are designed, the details of the resonant region characteristics are to be worked out. These details are schematically depicted in Fig. 6(a). In accordance with the abovementioned strategy, the radius of the two innermost waveguide sections (forming the central waveguide region in Fig. 6(a)) should be r_1 = 110 nm. In this manner, the lower edge of the photonic gap of the central waveguide coincides with the desired resonance wavelength $\lambda_0 = 1550$ nm. This is also shown in Fig. 5, where the band structure of the central waveguide region is depicted by dashed line.

The outer PC waveguide sections form a transitional waveguide region connecting the central waveguide region to PC waveguide mirrors. Determination of the air hole radii of the transitional waveguide region is the most difficult step. This step is carried out by using the proposed TL model of the structure shown in Fig. 6(b). To support a Gaussian electromagnetic field profile within the resonant region, the voltage distribution should follow a Gaussian pattern. The appropriate Gaussian voltage distribution for the PCNBR of Fig. 6(a) is depicted in Fig. 6(c). It can be easily shown that the following ratio is to be held:

$$\left|\frac{V_{n+1}}{V_n}\right| = \exp\left[-\frac{(n+1)^2a^2}{\sigma^2}\right] \Big/ \exp\left[-\frac{n^2a^2}{\sigma^2}\right] = \exp\left[-\frac{(2n+1)a^2}{\sigma^2}\right] \quad n = 2, \ldots, N \tag{8}$$

where σ is the standard deviation of the Gaussian profile and N is the number of the PC waveguide sections within each transitional region. It is worth noting that even though large σ is desirable because it results in large N and thus increases the quality factor by decreasing the radiation loss, we cannot increase σ beyond a certain value because by doing so we increase the mode volume of the resonant mode. A typical value at the resonance wavelength $\lambda_0 = 1550$ nm is $\sigma = 2$ μm.

Given that the ratio of the forward and backward waves within nth TL sections can be written as $V_n^+/V_n^- = (z_{c,n} - z_{c,n-1})/(z_{c,n} + z_{c,n-1})$, equation (8) can be further simplified and be written in terms of the characteristic impedance and propagation constant of the $(n-1)$th and nth TL sections

$$\left|\frac{z_{c,n}\cosh\gamma_{c,n}a + z_{c,n-1}\sinh\gamma_{c,n}a}{z_{c,n}}\right| = \exp\left[-\frac{(2n+1)\,a^2}{\sigma^2}\right] \quad n = 2, \ldots, N. \tag{9}$$

Fortunately, the characteristic impedance and the propagation constant of the TL model representing the central waveguide region is already known, and thus the characteristic impedance and the propagation constant of the remaining TL models can be easily determined in a recursive manner. Each of iterations has a search step therefore a database of propagation constants and characteristic impedances for a number of TL segments should be prepared. Starting from $n = 2$ in equation (9) which corresponds to closest PC waveguide section to the central PC waveguide section, we search the database for the TL segment (PC waveguide section) whose characteristic impedance and propagation constant satisfies equation (9). Then the same procedure should be repeated for the next segment ($n = 3$) and so forth. The recursive algorithm is terminated when the characteristic impedance and the propagation constant of one of the outer waveguide sections is close enough to the characteristic impedance and the propagation constant of the PC waveguide

TABLE I
RADII OF AIR HOLES IN THE TRANSITIONAL REGION OF THE DESIGNED PCNBR

Air Hole Number	Radius
r_2	109.8
r_3	109.3
r_4	108.4
r_5	107.2
r_6	105.6
r_7	103.7
r_8	101.4
r_9	98.7
r_{10}	95.7
r_{11}	92.4
r_{12}	88.7
r_{13}	84.7

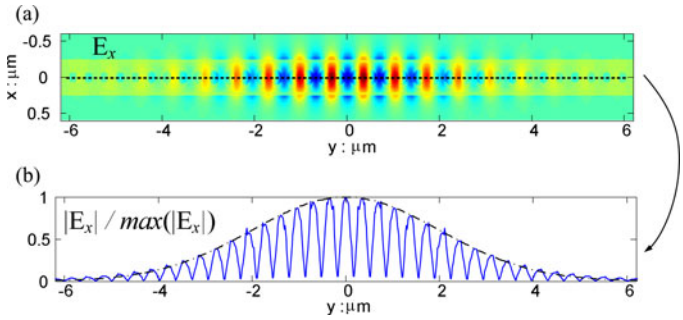

Fig. 7. (a) A snapshot of the x component of the electric field profile (E_x) of the resonance mode extracted from 3-D FDTD for a PCNBR with photonic crystal waveguide mirrors that are composed of 15 unit cells. (b) The absolute value of E_x in $x = 0$ along the resonator (blue solid line) and a Gaussian distribution with the standard deviation of $\sigma = 2\ \mu$m (dashed-dotted black line).

mirror. The difference is expected to be below 1%. In following example we have used a database of 30 different PC waveguide sections with air hole radiuses ranging from 110 to 80 nm.

Numerical calculations shows that for $w = 500$ nm, $h = 240$ nm, $t = 50$ nm, $\sigma = 2\ \mu$m, $r_m = 80$ nm, and $r_1 = 110$ nm, the transitional region should be made of 12 waveguide sections whose radii of air holes are tabulated in Table I.

To demonstrate that the designed PCNBR has a Gaussian filed profile, the FDTD simulation is employed to analyze the structure when the PC waveguide mirrors are composed of 15 unit cells. The resonance wavelength and the quality factor of the structure are 1566.48 nm, and 1.46×10^6, respectively (difference between resonance wavelength and quality factor calculated by using the proposed TL model and results of FDTD simulations is less that 0.1% and 5%, respectively). In Fig. 7(a) snap shot of the x component of the resonant electric field profile E_x is plotted together with its absolute value at $x = 0$ and $z = 0$. For the sake of comparison, a Gaussian envelop with the standard deviation of $\sigma = 2\ \mu$m is also plotted in Fig. 7(b). The similarity between the desired Gaussian profile and the actual shape of the electric field is striking.

It is worth noting that the high level of the quality factor of the designed PCNBR can be partly attributed to the rather large number of unit cells in the PC waveguide mirror section. Unfortunately, having large number of unit cells in the mirror section decreases the coupling efficiency and increases the device foot print. The transmission efficiency of the designed PCNBR in the direct coupling arrangement is below 4% (calculated by using proposed TL model). This is too low to be of practical importance. To improve the transmission efficiency, the same PCNBR with only six unit cells in the PC waveguide mirror section is considered. From TL model the resonance wavelength, the quality factor, and the transmission efficiency of this structure in the direct coupling arrangement are 1566.82 nm, 33900, and 33%, respectively. Although the quality factor of the structure is lowered, it is still high enough for miscellaneous applications. The transmission efficiency of the structure in the direct coupling arrangement; on the other hand, is considerably increased. The transmission efficiency can be further improved without deteriorating the quality factor of the structure. To this end, the radii of the air holes in the mirror section should be gradually decreased. But the gradual decrement of the air hole radii should be done in such a manner that no sharp transition be imposed on the electromagnetic field profile. Therefore, the same recursive formula should be used to guarantee the Gaussian field distribution. In this way, the PC waveguide mirror section in its original form is removed while the transitional region is extended. Since the lowest air hole radius that our fabrication process can realize with acceptable quality is about 50 nm, the air hole radii of the six unit cell sections in the extended transitional region are $r_{m1} = 80.5$ nm, $r_{m2} = 75.5$ nm, $r_{m3} = 70.5$ nm, $r_{m4} = 65.0$ nm, $r_{m5} = 59.0$ nm, and $r_{m6} = 53.0$ nm. These values are obtained by using equation (9). TL model based calculations show transmission efficiency of 96% for this PCBNR. It worth noting that while calculating transmission efficiency with 3-D FDTD simulation is a time consuming task (nearly impossible for ultra-high quality factor PCNBRs [10]) TL model can be used to directly calculate the transmission efficiency of PCNBRs. From the theory of microwave networks we know that each TL section with characteristic impedance z_c, propagation constant γ, and length l, can be represented by a transmission matrix (T-matrix). The T-matrix of a network made of cascaded TL sections $T_{\rm tot}$ can be calculated by multiplying the T-matrices of subsequent TL sections. Once the overall T-matrix of the PCNBR structure is obtained by multiplication of the T-matrix of PC waveguide sections, the transmission efficiency of the PCNBR can be calculated straightforwardly.

In previous studies ultra-high quality factor PCNBRs are designed based on air bridge dielectric waveguide or dielectric waveguides without pedestal [6], [15]. In this paper we have focused on designing high quality factor PCBNRs based on silicon rib waveguides. Presence of a 50 nm pedestal layer in the rib waveguide increases the radiation loss of the structure and therefore decreases the quality factor of designed PCNBRs. This radiation loss is why the qualify factor of the designed PCNBRs is lower than the quality factor of the PCNBRs reported in [6], [15]. It is by the way worth noting that extraction of the quality factor and the resonance wavelength by using the proposed approach remains valid as long as the quality factor of the PCNBR is in between 10^6 and 10^3. Besides, PCNBRs with low quality factor suffer from radiation loss, which is not properly modeled by the TL model. The quality factor cannot be too high because otherwise the FDTD simulations needed for extraction

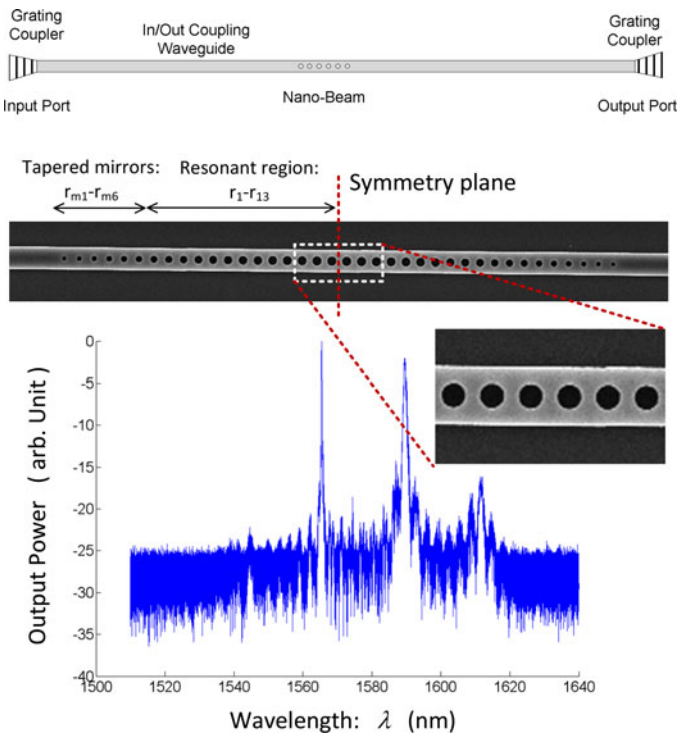

Fig. 8. Direct coupling scheme, characterization curve, and SEM image of the direct coupled nano-beam.

of the TL model parameters becomes very time consuming. One other important point is that the TL model considers one fundamental mode only. Therefore, the overall behavior of the structure should be dictated by the fundamental mode of the structure. In other words, higher order modes supported by the PC waveguide sections should remain below cut-off. Obviously, the PC waveguide cannot be multi-mode.

IV. Fabrication and Characterization Results

PCNBR designed in the last section is formed by perforating 13 pairs of air holes (with radii $r_1 - r_{13}$ given in Table I) as the resonant region and 6 air holes (with radii $r_{m1} - r_{m6}$ given in the previous section) as each mirror section in a silicon rib waveguide with a 50 nm pedestal layer (see Fig. 8). The PCNBR has been fabricated on a standard SOI wafer with 3 micron BOX and 240 nm top silicon layer. Patterns were defined by electron beam lithography (EBL) using 6% HSQ resist, spun at 5000 r/min for 60 s followed by prebaked at 90° for 3 min. After developing the EBL resist in 25% TMAH at an elevated temperature for 30 s, top silicon layer was dry etched by inductively coupled plasma tool using chlorine chemistry. The etching step is carefully controlled to etch 190 nm of the top Si layer and keep a pedestal layer with a thickness of 50 nm.

For characterization, the transmission spectrum over the wavelength range from 1510 to 1640 nm was measured using a wideband tunable laser and using a set of grating couplers to couple light to the PCNBR input/output waveguides. To improve the coupling efficiency from the input/output ridge waveguide to the PCNBR the air holes in the mirror section (at the intersection of the input/output waveguides and the PCNBR) have been appropriately tapered and hence extinction of about 25 dB was achievable for the first mode. Fig. 8 shows the schematic diagram of device, the transmission spectrum, and the micro-graphs of the fabricated PCNBR. Two peaks have been observed in the transmission response centered at $\lambda_0 = 1564.2$ nm and at $\lambda_0 = 1589.2$ nm with quality factors of 25000 and 4000, respectively. The measured quality factors of both modes are in good agreement with the prediction of the proposed model and also FDTD simulation (see Table II).

TABLE II
Characterization, FDTD, and TL Model Results for Direct Coupled Nano-Beams

	First Mode	Second Mode
Model	1567.10nm / 25300	1586.50nm / 4180
FDTD	1566.82nm / 25200	1585.00nm / 4150
Fabrication	1564.20nm / 25000	1589.20nm / 4000

V. Conclusion

We proposed a TL model for photonic crystal waveguide section and successfully used this model to design high quality factor PCNBR. This model provides an insight to silicon cavity design which significantly expedites simulation runtime. One particular PCNBR was designed to have maximum quality factor with a specific mode volume and resonance wavelength. The design procedure was based on realizing Gaussian field profile within the resonant region. Measurements show the excellent accuracy of the model in the estimation of the PCNBR resonance wavelength and quality factor.

References

[1] M. Belotti, M. Galli, D. Gerace, L. Andreani, G. Guizzetti, A. MdZain, N. Johnson, M. Sorel, and R. De La Rue, "All-optical switching in silicon-on-insulator photonic wire nano-cavities," *Opt. Exp.*, vol. 18, no. 2, pp. 1450–1461, Jan. 2010.

[2] B. Schmidt, Q. Xu, J. Shakya, S. Manipatruni, and M. Lipson, "Compact electro-optic modulator on silicon-on-insulator substrates using cavities with ultra-small modal volumes," *Opt. Exp.*, vol. 15, no. 6, pp. 3140–3148, Mar. 2007.

[3] R. Ohta, Y. Ota, M. Nomura, N. Kumagai, S. Ishida, S. Iwamoto, and Y. Arakawa, "Strong coupling between a photonic crystal nanobeam cavity and a single quantum dot," *Appl. Phys. Lett.*, vol. 98, no. 17, pp. 173104-1–173104-3, Apr. 2011.

[4] M. Eichenfield, R. Camacho, J. Chan, K. J. Vahala, and O. Painter, "A picogram- and nanometre-scale photonic-crystal optomechanical cavity," *Nature*, vol. 459, pp. 550–555, May 2009.

[5] P. B. Deotare, M. W. McCutcheon, I. W. Frank, M. Khan, and M. Loncar, "High quality factor photonic crystal nanobeam cavities," *Appl. Phys. Lett.*, vol. 94, no. 12, pp. 121106-1–121106-3, Mar. 2009.

[6] E. Kuramochi, H. Taniyama, T. Tanabe, K. Kawasaki, Y. Roh, and M. Notomi, "Ultrahigh-Q one-dimensional photonic crystal nanocavities with modulated mode-gap barriers on SiO2 claddings and on air claddings," *Opt. Exp.*, vol. 18, no. 15, pp. 15859–15869, Jul. 2010.

[7] J. D. Ryckman and S. M. Weiss, "Low mode volume slotted photonic crystal single nanobeam cavity," *Appl. Phys. Lett.*, vol. 101, no. 7, pp. 071104-1–071104-3, Aug. 2012.

[8] M. Notomi, E. Kuramochi, and H. Taniyama, "Ultrahigh-Q nanocavity with 1D photonic gap," *Opt. Exp.*, vol. 16, no. 15, pp. 11095–11102, Jul. 2008.

[9] M. McCutcheon and M. Loncar, "Design of a silicon nitride photonic crystal nanocavity with a quality factor of one million for coupling to a diamond nanocrystal," *Opt. Exp.*, vol. 16, no. 23, pp. 19136–19145, Nov. 2008.

[10] Q. Quan, P. B. Deotare, and M. Loncar, "Photonic crystal nanobeam cavity strongly coupled to the feeding waveguide," *Appl. Phys. Lett.*, vol. 96, no. 20, pp. 203102–203104, May 2010.

[11] Y. Gong, B. Ellis, G. Shambat, T. Sarmiento, J. Harris, and J. Vuckovic, "Nanobeam photonic crystal cavity quantum dot laser," *Opt. Exp.*, vol. 18, no. 9, pp. 8781–8789, Apr. 2010.

[12] Y. Zhang, M. Khan, Y. Huang, J. Ryou, P. Deotare, R. Dupuis, and M. Loncar, "Photonic crystal nanobeam lasers," *Appl. Phys. Lett.*, vol. 97, no. 5, pp. 051104–051106, Aug. 2010.

[13] B. Ahn, J. Kang, M. Kim, J. Song, B. Min, K. Kim, and Y. Lee, "One-dimensional parabolic-beam photonic crystal laser," *Opt. Exp.*, vol. 18, no. 6, pp. 5654–5660, Mar. 2010.

[14] P. Velha, J. C. Rodier, P. Lalanne, J. P. Hugonin, D. Peyrade, E. Picard, T. Charvolin, and E. Hadji, "Ultra-high-reflectivity photonic-bandgap mirrors in a ridge SOI waveguide," *New J. Phys.*, vol. 8, no. 9, p. 204, Sep. 2006.

[15] Q. Quan and M. Loncar, "Deterministic design of wavelength scale, ultra-high Q photonic crystal nanobeam cavities," *Opt. Exp.*, vol. 19, no. 19, pp. 18529–18542, Sep. 2011.

[16] P. Velha, E. Picard, T. Charvolin, E. Hadji, J. Rodier, P. Lalanne, and D. Peyrade, "Ultra-high Q/V Fabry–Perot microcavity on SOI substrate," *Opt. Exp.*, vol. 15, no. 24, pp. 16090–16096, Nov. 2007.

[17] A. Md Zain, N. Johnson, M. Sorel, and R. De La Rue, "Ultra high quality factor one dimensional photonic crystal/photonic wire micro-cavities in silicon-on-insulator (SOI)," *Opt. Exp.*, vol. 16, no. 16, pp. 12084–12089, Aug. 2008.

[18] M. Miri, A. Khavasi, K. Mehrany, and B. Rashidian, "Transmission-line model to design matching stage for light coupling into two-dimensional photonic crystals," *Opt. Lett.*, vol. 35, no. 2, pp. 115–117, Jan. 2010.

[19] M. A. Miri, A. Khavasi, M. Miri, and K. Mehrany, "A transmission line resonator model for fast extraction of electromagnetic properties of cavities in two-dimensional photonic crystals," *IEEE Photon. J.*, vol. 2, no. 4, pp. 677–685, Aug. 2010.

[20] R. E. Collin, *Foundation for Microwave Engineering*. New York: McGraw-Hill, 1992.

[21] Y. Akahane, T. Asano1, B. S. Song, and S. Noda, "High-Q photonic nanocavity in a two-dimensional photonic crystal," *Nature*, vol. 425, pp. 944–947, Sep. 2003.

[22] K. Srinivasan and O. Painter, "Momentum space design of high-Q photonic crystal optical cavities," *Opt. Exp.*, vol. 10, no. 15, pp. 670–684, Jul. 2002.

Authors' biographies not available at the time of publication.